THE JOURNAL OF PHYSICAL CHEMISTRY B

ARTICLE

pubs.acs.org/JPCB

Aggregation Behaviors of Dodecyl Sulfate-Based Anionic Surface Active Ionic Liquids in Water

Jingjing Jiao,[†] Bin Dong,[†] Huina Zhang,[‡] Yingyuan Zhao,[†] Xiaoqing Wang,[†] Rui Wang,[†] and Li Yu*[,†]

[†]Key Laboratory of Colloid and Interface Chemistry, Shandong University, Ministry of Education, Jinan 250100, PR China

[‡]Guangxi Agricultural Vocational-Technical College, Nanning 530007, PR China

ABSTRACT: Halogen-free, low-cost alkyl sulfate-based surface active ionic liquids (SAILs), 1-butyl-3-methylimidazolium dodecyl sulfate ($[C_4mim][C_{12}SO_4]$), and *N*-butyl-*N*-methylpyrrolidinium dodecyl sulfate ($[C_4MP][C_{12}SO_4]$) were easily synthesized through ion exchange reaction. The aggregation behaviors of $[C_4mim][C_{12}SO_4]$ and $[C_4MP][C_{12}SO_4]$ in aqueous solution were investigated by surface tension, electric conductivity, and static fluorescence quenching. Both $[C_4mim][C_{12}SO_4]$ and $[C_4MP][C_{12}SO_4]$ have rather lower cmc, γ_{cmc} values and higher pC_{20}, π_{cmc} values than those reported for the traditional ionic surfactant, sodium dodecyl sulfate (SDS), and imidazolium-based SAIL, 1-dodecyl-3-methylimidazolium bromide ($[C_{12}mim]Br$), with the same hydrocarbon chain length. The thermodynamic parameters evaluated from electric conductivity measurements show that the micelle formation of $[C_4mim][C_{12}SO_4]$ and $[C_4MP][C_{12}SO_4]$ is entropy-driven in the temperature range investigated. Lower average aggregation number indicates that the micelles of two SAILs present much looser structure. It is found that both the nature and the ring type of counterions can affect the aggregation behavior in aqueous solution. ^1H NMR results of $[C_4mim][C_{12}SO_4]$ were used to further verify the mechanism of micelle formation. Hydration ability and steric hindrance of the imidazolium or pyrrolidinium counterion as well as the cooperative hydrophobic interaction of longer alkyl chain of $[C_{12}SO_4]$ anion and comparatively shorter alkyl chain of $[C_4mim]$ or $[C_4MP]$ cation are proposed to play critical roles in the aggregation of $[C_4mim][C_{12}SO_4]$ and $[C_4MP][C_{12}SO_4]$.

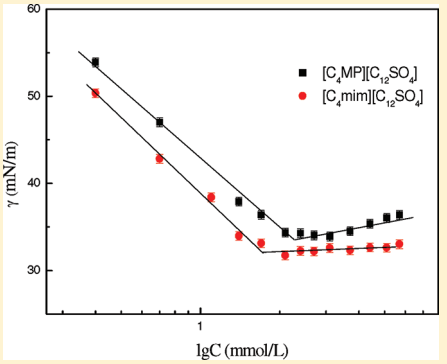

1. INTRODUCTION

Ionic liquids (ILs) are a class of organic molten electrolytes with the melting point lower than 100 °C, having attracted much attention due to their unique physicochemical properties, such as high ion conductivity and outstanding catalytic properties.[1−4] Many attempts have been made to construct functional ILs with specific properties.[5] ILs bearing long alkyl chains are found to have obvious amphiphilic characters and are named surface active ionic liquids (SAILs), one kind of functional ILs with combined properties of ILs and surfactants.[6] The aggregation behavior of SAILs in aqueous solutions has been a focus of recent investigations.[7−15] In addition, ILs are able to be designed and tuned to optimized yield. With the possibility of fine-tuning hydrophobicity of the ILs by changing the alkyl chain length, the type of headgroup, and the nature of the anions, one can change the structure of these aggregates.[16,17]

Most descriptions of SAILs in the literature focus too narrowly on the halogen-containing ILs. Even though they are environmentally benign compared to conventional organic solvent, the presence of halogen atoms might cause serious concerns if the anion is insufficiently stable regarding hydrolysis or if costly thermal treatments are needed to leave out release of corrosive HF or HCl.[18] So typical ILs consisting of halogen in anions limit their "greenness" in some ways. A number of halogen-free ILs with nitrate,[19] nitrite,[19] sulfate,[19] benzenesulfonate,[20] and toluenesulfonate anions[21] have been synthesized. Among them, alkyl sulfate-based ILs are clearly characterized by their high technical availability with relatively low cost and by their well-documented toxicology and biodegradation.[18,22,23] These make them particularly interesting candidates for expected future, industrial, bulk applications of ILs. For the first time, Wasserscheid et al. synthesized 1-butyl-3-methylimidazolium octyl sulfate ($[C_4mim][C_8SO_4]$).[18] Harjani et al. investigated the biodegradability of imidazolium ionic liquids paired with alkyl sulfate ions, including $[C_4mim][C_{12}SO_4]$. Miskolczy et al. studied the micelle formation of $[C_4mim][C_8SO_4]$ in aqueous solution through conductivity and turbidity measurements.[24] Arvind and his co-workers observed the dual micellar transitions in the aqueous solutions of $[C_4mim][C_8SO_4]$ by an array of techniques, such as conductivity, ^1H NMR, and 2D $^1H-^1H$ NOESY.[25]

A detailed survey of alkyl sulfate-based ILs indicates that most contributions have centered on $[C_4mim][C_8SO_4]$. In this work, halogen-free $[C_4mim][C_{12}SO_4]$ and $[C_4MP][C_{12}SO_4]$, derived from inexpensive chemicals, were synthesized using ion exchange, a method easier than that of the literature.[26] Their aggregation behaviors were studied systematically through surface tension measurement, conductivity measurement, and steady-state fluorescence quenching. In comparison with conventional ionic surfactant SDS and imidazolium-based SAIL $C_{12}mimBr$ sharing the same hydrophobic carbon chain, the uniqueness of

Received: September 26, 2011
Revised: December 21, 2011
Published: December 28, 2011

the nature of dodecyl sulfate-based anionic SAILs has been studied. The mechanism of micelle formation of alkyl sulfate-based SAILs was proposed based on the above experimental results and ^{1}H NMR spectra for [C_4mim][C_8SO_4].

2. EXPERIMENTAL SECTION

2.1. Materials. 1-Methylimidazole (99%) was purchased from Acros Organics. 1-Methyl pyrrolidine (98%) and butylchloride (98%) were obtained from Shanghai Aladdin Chemistry Co. Ltd. of China. Sodium dodecyl sulfate (SDS, 99.9%) and pyrene (99%) were purchased from Alfa Aesar. Benzophenone (chemical pure) was achieved from China Pharmaceutical Group. D_2O (99.9%) was bought from Sigma-Aldrich. All the reagents were used without further purification. Triply distilled water was used to prepare all the solutions.

2.2. Apparatus and Procedures. Surface tension measurements were carried out on the Tensiometer-K12 processor (Krüss Company, Germany) using the plate method. The surface tension was determined with a single measurement method. All measurements were repeated until the values were reproducible. Electrical conductivity measurements were employed on a low-frequency conductivity analyzer (Model DDSJ-308A, Shanghai Precision & Science Instrument Co., Ltd. of China). The temperature was controlled by a HAAKE DC30-K20 thermostatic bath (Karlsruhe, Germany). Each conductivity was recorded when its stability was better than 1% within 2 min. The steady-state fluorescence measurements were taken using a Perkin-Elmer fluorimeter LS-55 (U.S.). The fluorescence excitation wavelength was focused at 335 nm, the emission spectra wavelength ranged from 350 to 500 nm, and slit widths for emission and excitation were fixed at 2.5 and 10 nm, respectively.[27] Pyrene and benzophenone were used as fluorescence probe and quencher, respectively. The value of fluorescence intensity of pyrene was chosen at a wavelength of 273 nm. The concentrations of pyrene were fixed at 1×10^{-5} and 1×10^{-3} mol/L for [C_4mim]-[$C_{12}SO_4$] and [C_4MP][$C_{12}SO_4$], respectively. ^{1}H NMR spectra were carried out with a Bruker Avance 400 spectrometer at the frequency of 400.13 MHz at 25 ± 0.1 °C. Reproducibility of the results was confirmed by performing at least two experiments for each sample. Uncertainty for the chemical shift values was less than 10^{-3} ppm. All the surface tension, fluorescence spectra, and ^{1}H NMR spectra measurements were carried out at 25 ± 0.1 °C.

2.3. Synthesis of Ionic Liquids. 1-Butyl-3-methylimidazolium chloride ([C_4mim]Cl) and *N*-butyl-*N*-methylpyrrolidinium chloride (C_4MPCl) were prepared and purified according to procedures described elsewhere.[30] 1-Butyl-3-methylimidazolum dodecyl sulfate ([C_4mim][$C_{12}SO_4$]) was obtained by ion exchange reaction of [C_4mim]Cl and SDS. [C_4mim]Cl and SDS were stirred in dichloromethane at room temperature for 4 h, and the precipitation was removed by filtration. Then the organic phase was washed with water until the water was chloride-free (tested by titration with $AgNO_3$ from an acidic aqueous solution), and a white waxy solid [C_4mim][$C_{12}SO_4$] was obtained. *N*-butyl-*N*-methylpyrrolidinium dodecyl sulfate ([C_4MP][$C_{12}SO_4$]) was synthesized following the similar procedure. The final products were dried in vacuo for 48 h. The structures were ascertained by ^{1}H NMR spectroscopy with a Bruker Avance 300 spectrometer. And the ^{1}H NMR peak of D_2O (δ = 4.710 ppm) was used as the reference in determining the proton chemical shifts for [C_4mim][$C_{12}SO_4$] and [C_4MP][$C_{12}SO_4$]. For [C_4mim]-[$C_{12}SO_4$], ^{1}H NMR (δ/ppm): 8.62 (s, 1H, NCHN), 7.35, 7.31 (ss, 2H, NCH), 4.06 (t, J = 7.05, 2H, NCH_2), 3.82 (t, J = 6.45, 2H, $SOCH_2$), 3.75 (s, 3H, NCH_3), 1.69 (m, J = 7.42, 2H, $NCCH_2$), 1.47 (ss, J = 6.6, 2H, $NCCCH_2$), 1.16 (m, J = 9, $SOCH_2(CH_2)_9$, 20H), 0.77 (t, J = 7.35, 3H, $NCCCCH_3$), 0.67 (two, J = 6.6, 3H, $SOC_{11}CH_3$). For [C_4MP][$C_{12}SO_4$], ^{1}H NMR (δ/ppm): 3.90 (t, J = 6 0.6, 2H, $SOCH_2$), 3.41 (ss, J = 3, 4H, CH_2NCH_2), 3.22 (t, J = 8.55, 2H, NCH_2C), 2.94 (s, 3H, CH_3N), 2.11 (s, 4H, CCH_2CH_2C), 1.68 (m, J = 6.42, 2H, $NCCH_2C$), 1.55 (m, J = 6.9, 2H, $NCCCH_2C$), 1.30 (m, J = 7.5, 20H, $(CH_2)_{10}$), 0.87 (t, J = 7.35, 3H, $NCCCCH_3$), 0.77 (ss, J = 7.2, 3H, CH_3).

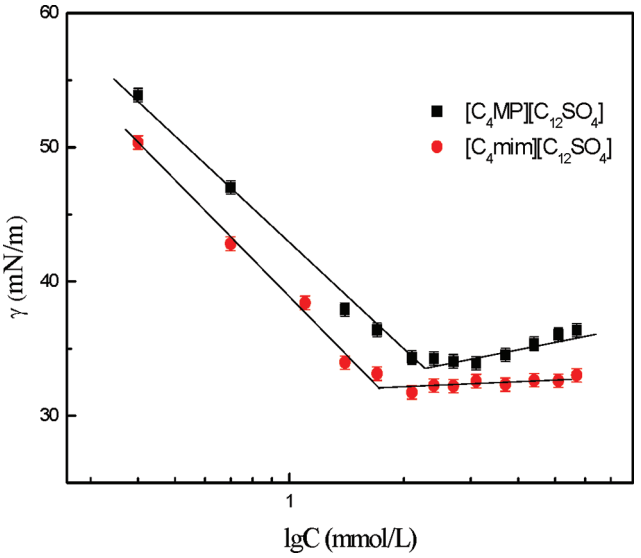

Figure 1. Surface tension as a function of log C for [C_4mim][$C_{12}SO_4$] (●) and [C_4MP][$C_{12}SO_4$] (■) at 25 °C.

3. RESULTS AND DISCUSSION

3.1. Surface Properties and Micellization Parameters. Surface tension measurements were performed to evaluate the surface activities of synthesized SAILs in aqueous solution. The plots of surface tension (γ) at 25 °C versus log C for [C_4mim][$C_{12}SO_4$] and [C_4MP][$C_{12}SO_4$] are depicted in Figure 1. The surface tension of aqueous solutions linearly decreases with the logarithm of concentration to a certain value, above which a nearly constant value of surface tension (γ_{cmc}) is observed. The absence of a minimum around the breakpoint demonstrates the high purities of these SAILs. The breakpoint between the two regions corresponds to the critical micelle concentration (cmc) value.

The cmc and γ_{cmc} values for [C_4mim][$C_{12}SO_4$] and [C_4MP]-[$C_{12}SO_4$] are listed in Table 1, together with the data reported for SDS,[29,30] [C_{12}mim]Br,[31] and *N*-dodecyl-*N*-methylpyrrolidimium bromide (C_{12}MPB)[32] which have the same hydrophobic chain length. It is evident that both [C_4mim][$C_{12}SO_4$] and [C_4MP][$C_{12}SO_4$] have rather lower cmc and γ_{cmc} than SDS, [C_{12}mim]Br, and C_{12}MPB suggesting that the SAILs studied have superior surface activity than the traditional ionic surfactant and imidazolium- or pyrrolium-based SAILs. Both electrostatic interaction and hydrophobic interaction can contribute to the formation of micelle and adsorption at the air−water interface.[33] So this difference can be ascribed to the following two reasons. On one hand, the weaker hydration of the bulky imidazolium or

dx.doi.org/10.1021/jp209276c |J. Phys. Chem. B 2012, 116, 958–965

Table 1. Surface Properties of $[C_4mim][C_{12}SO_4]$, $[C_4MP][C_{12}SO_4]$, SDS, and $[C_{12}mim]Br$ in Aqueous Solution at 25 °C

	cmc (mmol/L)	pC20	γ_{cmc} (mN/m)	A_{min} (nm^2)	Γ_{max} (μmol/m2)	π_{cmc} (mN/m)
$[C_4mim][C_{12}SO_4]$	1.8 ± 0.1	3.4 ± 0.109	31.9 ± 0.1	0.66 ± 0.071	2.53 ± 0.274	40.3 ± 0.1
$[C_4MP][C_{12}SO4]$	2.7 ± 0.1	3.5 ± 0.137	34.3 ± 0.1	0.74 ± 0.026	2.27 ± 0.079	37.9 ± 0.1
SDS[a]	7.8	2.4	39.6	0.48	3.45	32.5
$C_{12}mimBr$[b]	10.9	2.6	39.4	0.87	1.91	33.6
$C_{12}MPB$[c]	13.5	–	42.4	0.55	3.03	30.3

[a] Reported in ref 28. [b] Reported in ref 31. [c] Reported in ref 32.

pyrrolidinium counterions makes the reduction of the electrostatic repulsion between headgroups more effective and in this way facilitates the micelle formation. On the other hand, the butyl on the imidazolium or pyrrolidinium ring for $[C_4mim][C_{12}SO_4]$ or $[C_4MP][C_{12}SO_4]$ might intersperse in the region of the dynamic equilibrium micelle as the short carbon chain of $[C_4mim]^+$ could penetrate in the fence layers of the micelles in the mixture of $[C_4mim]PF_6$ and SDS.[34] It plays a role similar to that of the second hydrophobic chain (i.e., butyl on the counterion ring) when micelles are formed, and thus the cmc value becomes smaller. Compared with $[C_4MP][C_{12}SO_4]$, the smaller cmc and γ_{cmc} of $[C_4mim][C_{12}SO_4]$ can be attributed to the delocalized positive charge on the imidazolium ring and the ubiquitous hydrogen bonds among the imidazolium cations,[35,36] which can reduce the electrostatic repulsion of the alkyl sulfate headgroups and thus promote the micelle formation.

In addition, Miskolczy et al. showed that 1-butyl-3-methylimidazolium octyl sulfate ($[C_4mim][C_8SO_4]$) can form micelles in aqueous solution and its cmc was 31 mmol/L, which is higher than that of $[C_4mim][C_{12}SO_4]$. This can be ascribed to the more hydrophobic property of the latter which has a longer hydrocarbon tail. What's more, it is very interesting that the cmc value of $[C_4mim][C_{12}SO_4]$ is about a quarter of that for SDS, and so are $[C_4mim][C_8SO_4]$ and sodium octyl sulfate (SOS). The large $[C_4mim]^+$ cation is more effective at screening the intramicellar electrostatic repulsion among the polar headgroups allowing signifcantly lower cmc value for 1-butyl-3-methylimidazolium alkyl sulfate compared with the cmc value of alkyl sulfate sodium with the identical hydrocarbon tails.

Based on the surface tension plots, two additional parameters, i.e., the effectiveness of surface tension reduction, π_{cmc}, and the adsorption efficiency, pC_{20} were estimated. π_{cmc} indicates the maximum reduction of surface tension caused by the dissolution of surfactant molecules and hence becomes a measure for the effectiveness of the surfactant to lower the surface tension of the solvent.[37] pC_{20} is used to explain the ability of decreasing surface tension for surfactant. As listed in Table 1, both pC_{20} and π_{cmc} values for $[C_4mim][C_{12}SO_4]$ and $[C_4MP][C_{12}SO_4]$ are much higher than those of SDS and $[C_{12}mim]Br$, which reveals their more excellent activity than SDS and $[C_{12}mim]Br$ in decreasing surface tension of water. This difference is probably due to the bulky size of pyrrolidinium and imidazolium counterions, which can be less hydrated by water and strongly attach to the alkyl sulfate anion and subsequently reduce the electrostatic repulsion between headgroups. The slightly higher π_{cmc} value of $[C_4MP][C_{12}SO_4]$ than $[C_4mim][C_{12}SO_4]$ may be due to the higher hydrophobic tendency for pyrrolidinium cation than imidazolium cation.[38]

The maximum surface excess concentration, Γ_{max}, and the area occupied by a single surfactant molecule at the air−liquid interface, A_{min}, reflect the arrangement of surfactant molecules at the air−liquid interface. They were estimated according to Gibbs adsorption isotherm.[39,40] Table 1 shows the obtained Γ_{max} and A_{min} values for $[C_4mim][C_{12}SO_4]$, $[C_4MP][C_{12}SO_4]$, SDS, $[C_{12}mim]Br$, and $C_{12}MPB$. The values of Γ_{max} increase in the order $[C_{12}mim]Br < [C_4MP][C_{12}SO_4] < [C_4mim][C_{12}SO_4] < C_{12}MPB <$ SDS, while the A_{min} values reduce in the same order. As reported,[41] bigger Γ_{max} or smaller A_{min} means a denser arrangement of surfactant molecules at the surface of the solution. It is well established that the structure of hydrophilic headgroup is a dominant factor in the determination of Γ_{max} and A_{min} values of surfactants.[41] So compared with imidazolium-based SAILs, the

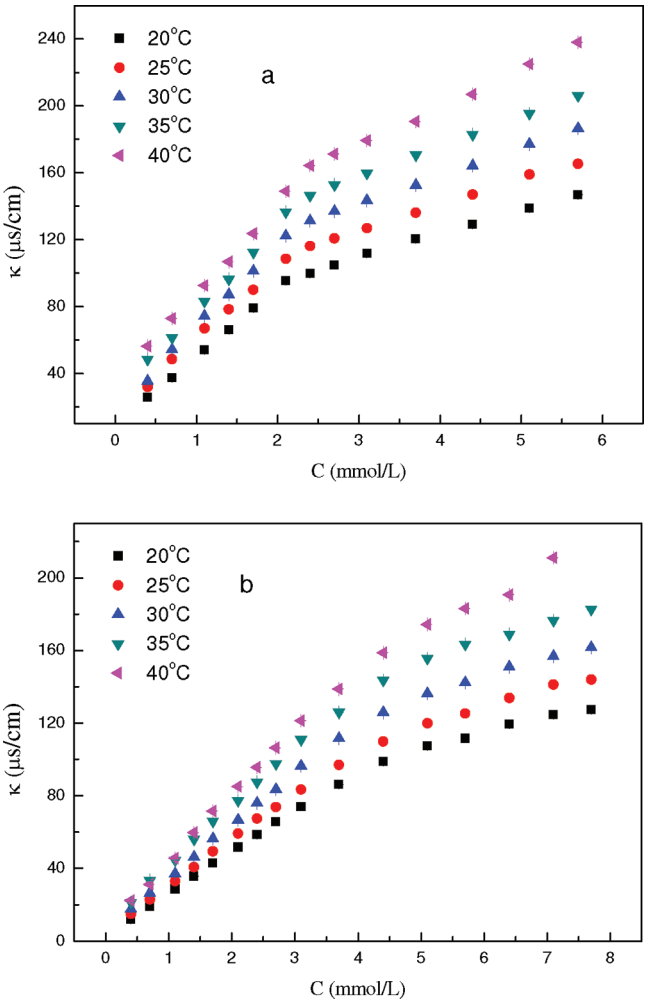

Figure 2. Plots of electrical conductivity versus concentration of $[C_4mim][C_{12}SO_4]$ (a) and $[C_4MP][C_{12}SO_4]$ (b) at different temperatures.

dx.doi.org/10.1021/jp209276c |J. Phys. Chem. B 2012, 116, 958–965

Table 2. Critical Micelle Concentration (cmc), Degree of Counterion Binding (β), and Thermodynamic Parameters of Micelle Formation for $[C_4mim][C_{12}SO_4]$ and $[C_4MP][C_{12}SO_4]$ in Aqueous Solution at Different Temperatures

	T/°C	β	cmc (mmol/L)	ΔG (kJ/mol)	ΔH (kJ/mol)	$-T\Delta S$ (kJ/mol)
$[C_4mim][C_{12}SO_4]$	20	0.65 ± 0.01	2.1 ± 0.1	−41.06 ± 0.293	−4.89 ± 0.0337	−36.17 ± 0.259
	25	0.65 ± 0.01	2.1 ± 0.1	−41.71 ± 0.298	−5.05 ± 0.0348	−36.66 ± 0.263
	30	0.65 ± 0.01	2.2 ± 0.1	−42.40 ± 0.298	−5.21 ± 0.036	−37.19 ± 0.262
	35	0.66 ± 0.01	2.2 ± 0.1	−43.27 ± 0.303	−5.36 ± 0.0372	−37.91 ± 0.266
	40	0.67 ± 0.01	2.3 ± 0.1	−43.88 ± 0.303	−5.51 ± 0.0384	−38.37 ± 0.265
$[C_4MP][C_{12}SO_4]$	20	0.50 ± 0.01	3.7 ± 0.1	−35.11 ± 0.254	−3.83 ± 0.0316	−29.81 ± 0.222
	25	0.57 ± 0.01	3.8 ± 0.1	−37.27 ± 0.240	−3.96 ± 0.0327	−32.04 ± 0.207
	30	0.60 ± 0.01	3.9 ± 0.1	−38.68 ± 0.257	−4.09 ± 0.0338	−33.42 ± 0.223
	35	0.68 ± 0.01	4.0 ± 0.1	−41.12 ± 0.258	−4.23 ± 0.0349	−37.52 ± 0.223
	40	0.69 ± 0.01	4.1 ± 0.1	−41.89 ± 0.261	−4.37 ± 0.0360	−35.99 ± 0.225

bigger Γ_{max} value and smaller A_{min} obtained for alkyl sulfate-based SAILs can be mainly attributed to the smaller size of sulfate anion by comparison with the imidazolium cation. It seems that pyrrolidium-based SAILs have a similar rule as imidazolium-based SAILs. But it is not the case. Compared with alkyl sulfate-based SAILs with the same hydrophobic chain length, $C_{12}MPB$ has bigger Γ_{max} and smaller A_{min} values. Perhaps the higher hydrophobicity of pyrrolidinium cation has a significant effect on the hydrophilicity of the headgroup in comparion with the imidazolium cation.[42] But for the two SAILs studied in this work and SDS, the hydrophilic headgroup is identical and the counterion is different. This may be reasonable considering the bulkiness of both imidazolium and pyrrolidinium cations, compared to small counterions like Na^+, and hydrophobic character of the butyl on the imidazolium and pyrrolidinium rings. The lower A_{min} and higher Γ_{max} values for $[C_4mim][C_{12}SO_4]$ in contrast with $[C_4MP][C_{12}SO_4]$ suggest that it has a more compact structure at the air/water interface due to the greater solvation in water of the imidazolium cation.

3.2. Electrical Conductivity Measurement and Thermodynamic Parameters of Micelle Formation. Electrical conductivity measurements were employed to study the micellar aggregation behavior of the two SAILs in aqueous solutions at different temperatures. Figure 2 depicts the change of the electrical conductivity (κ) as a function of concentration of the $[C_4mim][C_{12}SO_4]$ and $[C_4MP][C_{12}SO_4]$ solutions in the temperature range of 20−40 °C. Each plot exhibits two straight lines with different slopes. The change of slope originates from the formation of micelles, and the junction of the two straight lines is assigned to the value of the cmc.[43] As given in Table 2, for $[C_4mim][C_{12}SO_4]$ and $[C_4MP][C_{12}SO_4]$, the cmc values at 25 °C obtained by this method are in good accordance with those determined by surface tension measurements (Table 1). All cmc values of $[C_4mim][C_{12}SO_4]$ and $[C_4MP][C_{12}SO_4]$ increase slightly with temperature increase, which is similar to the case for most ionic surfactants.[43−47] The cmc values of an ionic surfactant are affected by temperature because of two opposite processes. The increase in temperature weakens the hydration of the hydrophilic groups, which favors micelle formation and decreases cmc. However, the orderly structure of water molecules surrounding the hydrophobic groups is destroyed with increasing temperature, which is disadvantageous to the micelle formation and increases cmc.[32] The results indicate that the latter plays a main role in the micellar formation for the SAILs studied in this work.

Based on the mixed electrolyte model of micellar solution,[41] the degree of counterion dissociation (α) can be estimated from the ratio between the slopes of the electrical conductivity versus concentration plots above and below cmc. And the degree of counterion binding of micelle (β) can be obtained. The values of β for $[C_4mim][C_{12}SO_4]$ and $[C_4MP][C_{12}SO_4]$ at different temperatures are summarized in Table 2. Compared with SDS (β = 0.74[48]) and $[C_{12}mim]Br$ (β = 0.77[46]), both $[C_4mim][C_{12}SO_4]$ and $[C_4MP][C_{12}SO_4]$ have lower β values at 25 °C. This can be ascribed to the effect of counterion species, namely, smaller inorganic counterion (Na^+, Br^-) and larger cyclic organic counterions ($[C_4mim]^+$ and $[C_4MP]^+$). The steric hindrance reduces the interaction between the counterion and hydrophilic headgroup and results in less counterions existing at the micellar surface. Moreover, for $[C_4mim][C_{12}SO_4]$ and $[C_4MP][C_{12}SO_4]$, β values increase with the increasing temperature, possibly due to the fact that the weaker solvation of bulky pyrrolidinium or imidazolium counterions plays a predominant role over the stronger thermal movement. As a result, at higher temperature the attraction between the headgroup and counterion around the Stern layer is enhanced.

For the alkyl sulfate-based SAILs studied in this work, the weak change intensity of β values varying with temperature is synonymous to weak attraction between the headgroup and counterion around the Stern layer. There are two major interaction modes for the heterocyclic ring counterions to bind to micelles, commonly electrostatic and hydrophobic interactions. As reported,[42] for imidazolium series electrostatic interaction is more important, while for pyrrolidimium series hydrophobic interaction is dominant. As is well-known to all, compared to electrostatic interaction, hydrophobic interactions are more sensitive to temperature. So with the increasing temperature, hydrophobic interaction is considerably weakened but electrostatic interaction changes little. So variation of the degree of counterion binding of micelle for $[C_4mim][C_{12}SO_4]$ is smaller than that of $[C_4MP][C_{12}SO_4]$.

According to the pesudophase model of micellization, micellar thermodynamic parameters were estimated, the standard Gibbs free energy of micellization (ΔG_m^θ), the micellization standard enthalpy (ΔH_m^θ), and the micellization standard entropy (ΔS_m^θ). As listed in the Table 2, the negative value of (ΔG_m^θ) means that micellization of the studied SAILs in aqueous solution is a spontaneous process in the temperature range investigated. At each temperature, the value of (ΔG_m^θ) for $[C_4mim][C_{12}SO_4]$ is always more negative than that of $[C_4MP][C_{12}SO_4]$, suggesting that it is easier for the former to form micelle. The value of (ΔH_m^θ) is negative as well, indicating an exothermic micellization process. And the negative value of (ΔH_m^θ) is much lower than

dx.doi.org/10.1021/jp209276c |J. Phys. Chem. B 2012, 116, 958–965

that of $(-T\Delta S_m^{\theta})$, indicating that the micellization for the SAILs in aqueous solution is entropy-driven. So the driving force of the micellization process is the hydrophobic group of surfactant transfer from solution environment to interior of the micelle.[49] During this process, the solvated water molecules are released which results in entropy increase.

3.3. Static Fluorescence Quenching and Average Aggregation Number. The average aggregation number (N_{agg}) is a fundamental and important parameter of micelle aggregation[50] and can be investigated by static fluorescence quenching according to the Turro−Yekta method.[51] The main assumptions of this method are as follows. First, the quencher and probe are solubilized in the micelle phase completely. Second, the random distribution of the probe and quencher in the micelles obeys a Poisson distribution. In the present work, pyrene and benzophenone are used as the probe and quencher, respectively. Pyrene as a kind of oil-soluble material is dissolved in the interior of micelles. The adding of benzophenone decreases the fluorescence intensity of pyrene gradually. Thus N_{agg} can be obtained by applying the following equation to the fluorescence data

$$\ln\left(\frac{I_0}{I}\right) = \frac{N_{agg}c_Q}{c_S - \mathrm{cmc}} \quad (1)$$

where I_0 and I are fluorescence intensities of pyrene in the absence and presence of benzophenone, respectively, and C_Q and C_S are the concentrations of benzophenone and SAILs, respectively.

Figure 3 depicts the plots of logarithm of the pyrene intensity ratio (I_0/I) versus the concentration of benzophenone at 25 °C for $[C_4mim][C_{12}SO_4]$ and $[C_4MP][C_{12}SO_4]$. One can see a good linear relationship, and N_{agg} can be calculated by the slope of the lines according to eq 1. The N_{agg} value of $[C_4mim][C_{12}SO_4]$ (N_{agg} = 27) is larger than that of $[C_4MP][C_{12}SO_4]$ (N_{agg} = 18), but much smaller than those of SDS (N_{agg} = 55)[50] and $[C_{12}mim]Br$ (N_{agg} = 37).[32] This indicates that both $[C_4mim][C_{12}SO_4]$ and $[C_4MP][C_{12}SO_4]$ micelles present much looser structures. It can be attributed to the higher steric effects arising from the larger bulk organic pyrrodinium and imidazolium counterions. The reason for the higher aggregation number of $[C_4mim][C_{12}SO_4]$ by comparison with $[C_4MP][C_{12}SO_4]$ is that the electric repulsion interaction between the headgroups is more effectively reduced by imidazolium cation than pyrrolium cation. It helps to aggregate into micelles for monomers.

3.4. ^{1}H NMR Spectra. As a sensitive and accutate technique, NMR was used to investigate the aggregation behavior of surfactants in detail.[51−53] The ^{1}H NMR chemical shift observed (δ_{obsd}) of alkyl chains is very particularly sensitive to conformational changes occurring during the process of self-assembly or the restructuring of self-assembled structures.[54] Here $[C_4mim][C_{12}SO_4]$ was taken as an example to study the aggregation behavior by ^{1}H NMR. All protons of $[C_4mim][C_{12}SO_4]$ can be divided into two parts: protons on imidazolium cation (H_{a-h}) and protons on the dodecyl sulfate anion (H_{i-k}).

As a typical example, the protons assignments and ^{1}H NMR spectrum of 2.7 mmol/L $[C_4mim][C_{12}SO_4]$ in D_2O are presented in Figure 4. The change of chemical shift (δ) as a function of the concentration of $[C_4mim][C_{12}SO_4]$ in aqueous solution for all protons was carefully examined. The variation of the chemical shift of protons ($\Delta\delta = \delta_{obsd} - \delta_{mon}$) as a function of reciprocal concentration for various protons is depicted in Figure 5. Slight changes of the chemical shifts are observed below the cmc. At the cmc, the sharp change of chemical shift appears, indicating the change of environment, related to the formation of micelles.

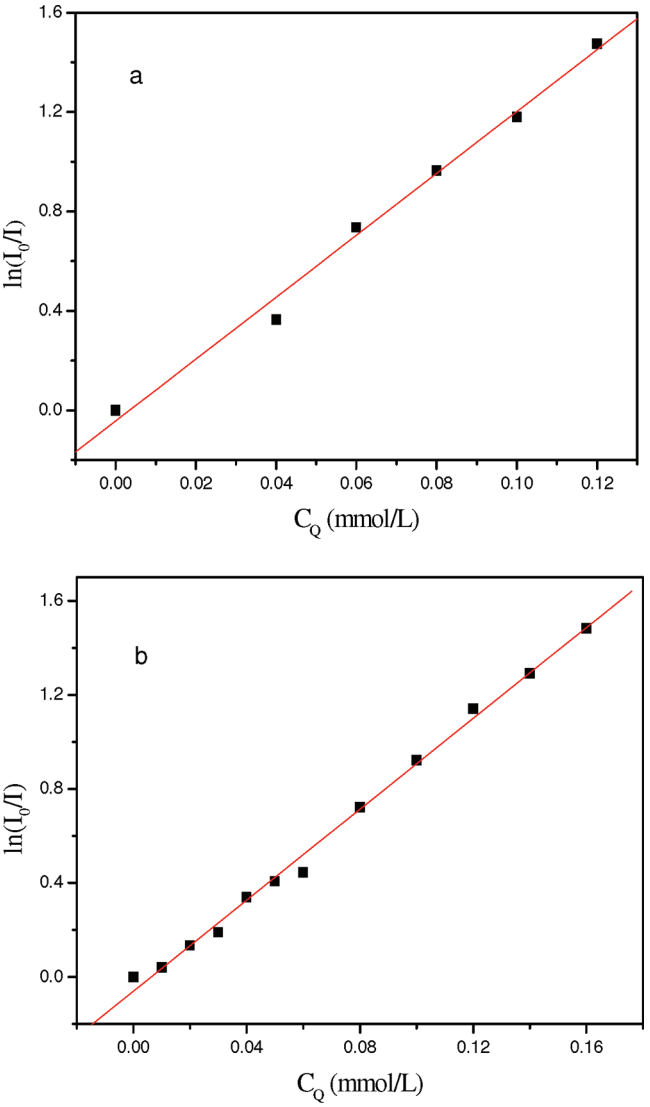

Figure 3. Value of $\ln(I_0/I)$ of pyrene as a function of concentration of benzophenone in the solution of $[C_4mim][C_{12}SO_4]$ at 4 mmol/L (a) and $[C_4MP][C_{12}SO_4]$ at 8 mmol/L (b).

Protons on imidazolium cation have a downfield shift; meanwhile, protons on alkyl chain have an upfield shift. Interestingly, H_f proton on the aromatic ring moves to upfield greatly. The magnitude change for $\Delta\delta$ must be generally affected by aromatic ring current, hydrogen bond, and solvent effect. The ring current effect has a quite rigorous geometrical restriction, and protons only located in the field of the ring are substantially shifted. The downshield shift for the protons of the imidazolium cation mainly results from the deshielding effect. Meanwhile, electron density of these protons on imidazolium cation is reduced due to contact with electronegative oxygen atoms of the anionic headgroup. Gradual decrease of $\Delta\delta$ toward the end of the alkyl chain on the imidazolium ring indicates that these protons are less influenced by the ring current and the anionic headgroup. This phenomenon further indicates a micellar mechanism in which

dx.doi.org/10.1021/jp209276c |J. Phys. Chem. B 2012, 116, 958–965

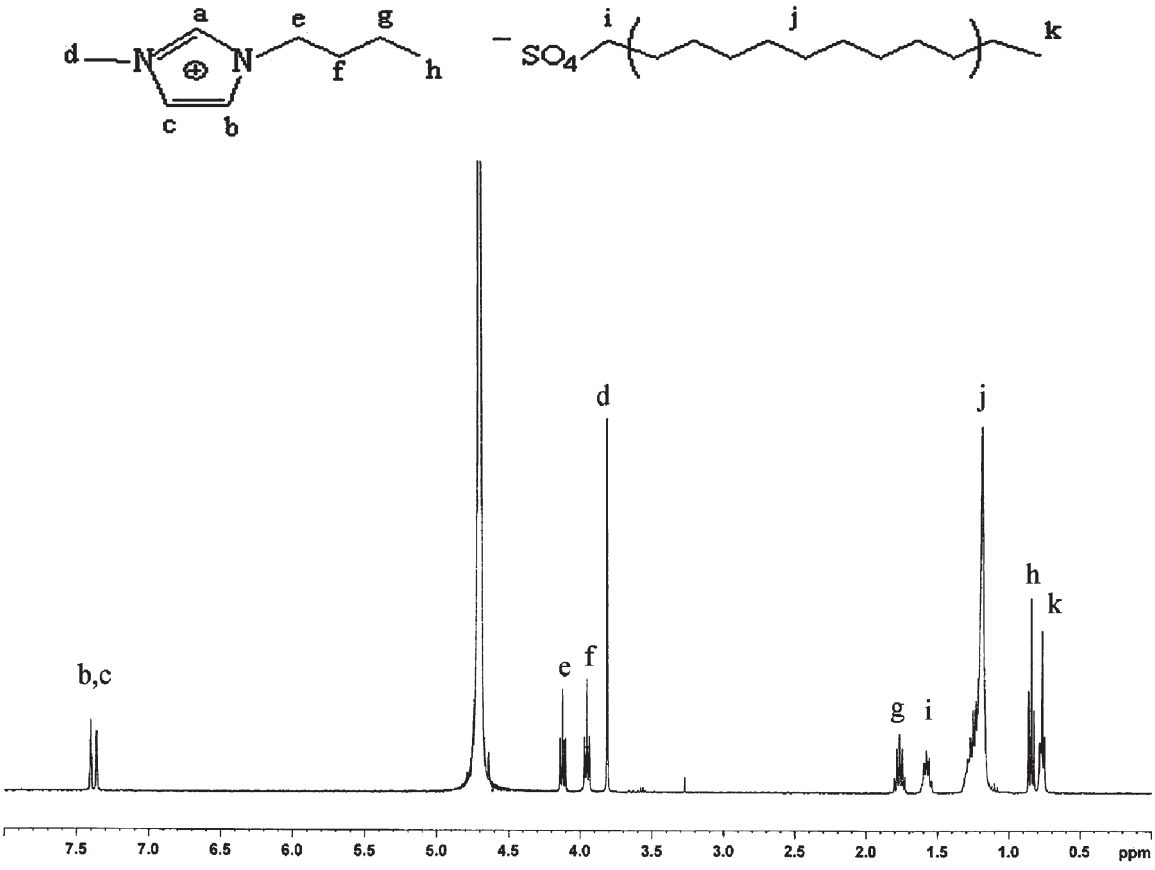

Figure 4. Proton assignments and 1H NMR spectrum of $[C_4mim][C_{12}SO_4]$ at concentration of 2.7 mmol/L in D_2O at 25 °C.

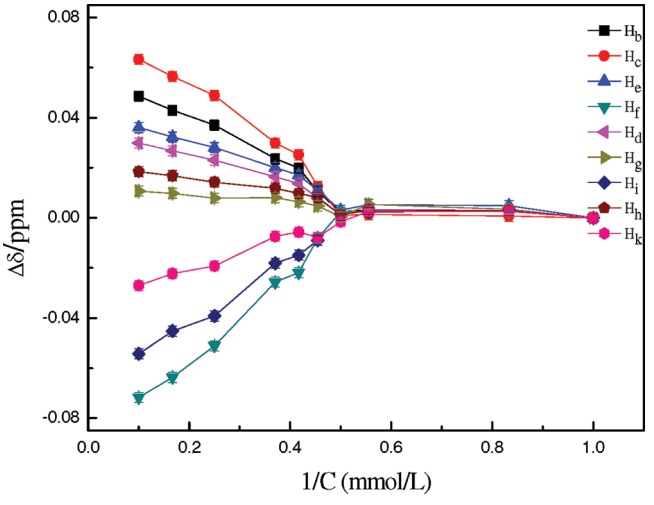

Figure 5. $\Delta\delta$ for various protons of $[C_4mim][C_{12}SO_4]$ at different concentrations in D_2O at 25 °C.

imidazolium cation contacts the negative headgroup of dodecyl sulfate located on the surface of micelle as shown in Figure 6. Pandey et.al. put forward a mechanism about micellization in the system of sodium dodecyl sulfate in the presence of $bmimPF_6$. With strong electrostatic attraction and hydrophobic interaction, $bmimPF_6$ is present in the proximity of the anionic micellar surface.[37] Hydrogen bonding is also a main factor to induce the chemical shift of protons toward downfield. There exist weaker intermolecular hydrogen bonds between D_2O and protons contacting directly to ring or on the hydrophobic methyl or butyl. When micelles begin to form, imidazolium cations as counterions approach the interface of dynamic micelles. Some D_2O molecules are replaced by dodecyl sulfate anion, and stronger intramolecular hydrogen bonds appear, which induces these protons to downfield shift. Great magnitude changes of chemical shift for H_b, H_c are the typical performance of hydrogen bond formation.

Dodecyl chain of the anion shows an upfield shift that can be related to the van der Waals interactions and the gauche conformation originating from changeover from the trans to the gauche conformation of the alkyl chain in aggregates formation.[54] While the shielding of aromatic ring current also might make H_i, H_k move toward upfield, H_i has an obvious change of chemical shift since it is close to the imidazolium cation during micelle formation. Interestingly, for the proton of H_f, different from other protons on the ring, it moves greatly toward upfield. The reason might be that when cation closes to anion, the conformational changes of butyl make a movement of H_f into the shielding region. The reversion from deshielding region to shielding region results in a distinct change in chemical shift.

The theory of pseudophase transition model considers that the chemical shift observed, δ_{obsd}, is a weighted average value of monomers (δ_{mon}) and micelles (δ_{mic}) according to the proportion in mole.[55]

$$\delta_{obsd} = \frac{C_{mon}}{C}\delta_{mon} + \frac{C_{mic}}{C}\delta_{mic} \quad (2)$$

where C_{mon}, C_{mic}, and C are the concentrations of surfactants existing as monomers, micelles, and the total concentration, respectively.

dx.doi.org/10.1021/jp209276c |J. Phys. Chem. B 2012, 116, 958–965

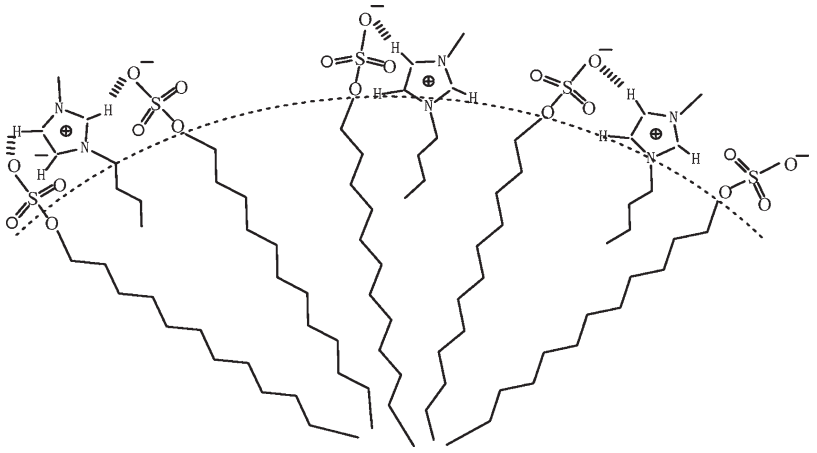

Figure 6. Scheme of micelle formation for $[C_4mim][C_{12}SO_4]$.

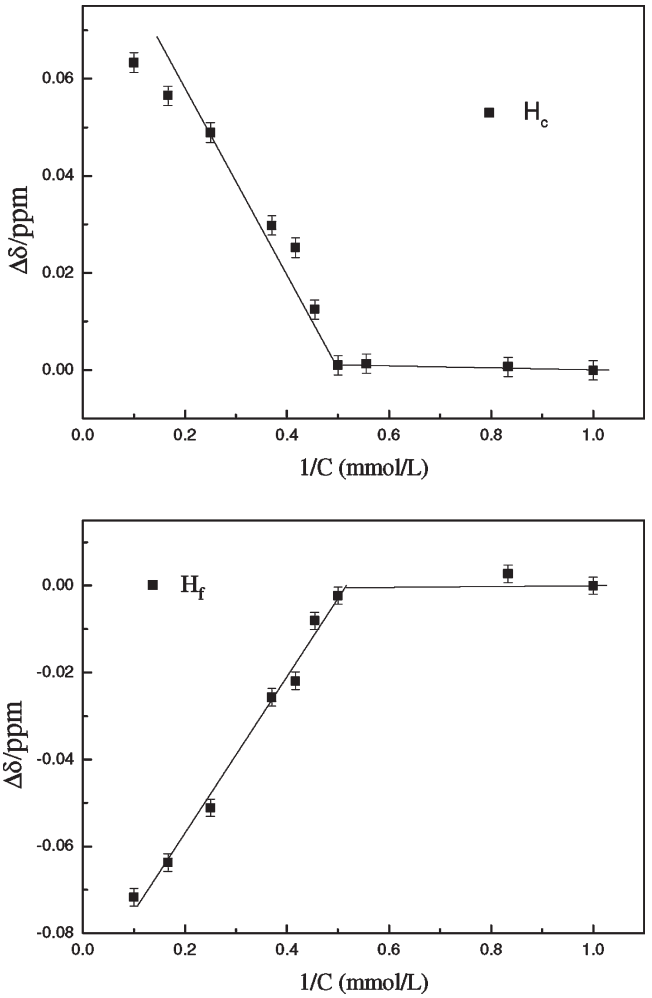

Figure 7. Variations for chemical shift $\Delta\delta$ for $[C_4mim][C_{12}SO_4]$ protons (H_c, H_f) versus the reciprocal concentration of ILs in D_2O at 25 °C.

When the concentration is above cmc, C_{mon} is assumed to be constant. So the eq 2 can be transformed as follows

$$\delta_{obsd} = \frac{cmc}{C}(\delta_{mon} - \delta_{mic}) + \delta_{mic} \quad (3)$$

Difference in the value between δ_{obsd} and δ_{mon} can be expressed as $\Delta\delta$, so

$$\Delta\delta = \frac{cmc}{C}(\delta_{mon} - \delta_{mic}) + \delta_{mic} - \delta_{mon} \quad (4)$$

The plots of $\Delta\delta$ versus $1/C$ for H_c, H_f are taken as examples and depicted in Figure 7. There are two straight lines with intersection corresponding to the cmc of $[C_4mim][C_{12}SO_4]$, 1.9 mmol/L, which is slightly lower than that of aqueous solution at 25 °C (Table 1 and Table 2). This results from the solvent D_2O, a more structured liquid.[56]

4. CONCLUSIONS

Halogen-free SAILs, $[C_4mim][C_{12}SO_4]$ and $[C_4MP][C_{12}SO_4]$, were synthesized as potential new surfactants. Their aggregation behaviors in aqueous solution were studied systematically by various techniques in fairly good agreement. The experimental results demonstrate that both $[C_4mim][C_{12}SO_4]$ and $[C_4MP][C_{12}SO_4]$ show good micelle characteristics superior to traditional surfactant sodium dodecyl sulfate (SDS) and imidazolium-based SAIL, $[C_{12}mim]Br$ and $C_{12}MPB$, with the same hydrophobic chain length, e.g., lower cmc and γ_{cmc} values. The ^1H NMR results for $[C_4mim][C_{12}SO_4]$ verified the mechanism of micelle formation and the micellar structure. Dodecyl aggregates into micelle while imidazolium cation contacts to anion headgroup on the surface of micelle and butyl on imidazolium cation penetrates into the micelle. Unique physicochemical properties, superior surface activity, and well-documented biodegradability turn the halogen-free alkyl sulfate-based SAILs to suitable candidates for different multiton-scale industrial applications. They can be exploited for utilizing as potential substitutes for conventional surfactants in various applications.

AUTHOR INFORMATION

Corresponding Author

*Phone number +86-531-88364807; fax number +86-531-88564750; e-mail address ylmlt@sdu.edu.cn.

ACKNOWLEDGMENT

This work was supported by the Natural Scientific Foundation of Shandong Province of China (No. ZR2011BM017 and

No. Z2007B03), Scientific and Technological Projects of Shandong Province of China (No. 2009GG10003027), and Independent Innovation Foundation of Shandong University (IIFSDU) of China (No. 2009TS018).

REFERENCES

(1) Rogers, R. D.; Seddon, K. R. *Science* **2003**, *302*, 792–793.
(2) Welton, T. *Chem. Rev.* **1999**, *99*, 2071–2083.
(3) Dyson, P. J.; Ellis, D. J.; Parker, D. G.; Welton, T. *Chem. Commun.* **1999**, 25–26.
(4) Anderson, J. L.; Ding, J.; Welton, T.; Armstrong, D. W. *J. Am. Chem. Soc.* **2002**, *124*, 14247–14254.
(5) Lee, S-g. *Chem. Commun.* **2006**, 1049–1063.
(6) El Seoud, O. A.; Pires, P. A. R.; Abdel-Moghny, T.; Bastos, E. L. *J. Colloid Interface Sci.* **2007**, *313*, 296–304.
(7) Bowers, J.; Craig, P.; Butts, P. J.; Martin, M. C.; Vergara-Gutierrez. *Langmuir* **2004**, *20*, 2191–2198.
(8) Bradley, A. E.; Hardacre, C.; Holbrey, J. D.; Johnston, S.; McGrath, S. E. J.; Nieuwenhuyzen, M. *Chem. Mater.* **2002**, *14*, 629–635.
(9) Goodchild, I.; Collier, L.; Millar, S. L.; Prokeš, I.; Lord, J. C. D.; Butts, C. P.; Bowers, J.; Webster, J. R. P.; Heenan, R. K. *J. Colloid Interface Sci.* **2007**, *307*, 455–468.
(10) Evans, D. F.; Yamauchi, A.; Wei, G. J.; Bloomfield, V. A. *J. Phys. Chem.* **1983**, *87*, 3537–3541.
(11) Evans, D. F.; Kaler, E. W.; Benton, W. J. *J. Phys. Chem.* **1983**, *87*, 533–535.
(12) Zhao, Y. R.; Chen, X.; Wang, X. D. *J. Phys. Chem. B.* **2009**, *113*, 2024–2030.
(13) Jiang, W. Q.; Hao, J. C.; Wu, Z. H. *Langmuir* **2008**, *24*, 3150–3156.
(14) Boy, M.; Voss, H. *J. Mol. Catal. B: Enzym.* **1998**, *5*, 355–359.
(15) Coldren, B.; Zanten, R. V.; Mackel, M. J.; Zasadzinski, J. A. *Langmuir* **2003**, *19*, 5632–5639.
(16) Singh, T.; Kumar, A. *J. Phys. Chem. B.* **2007**, *111*, 7843–7851.
(17) Wang, H. Y.; Wang, J. J.; Zhang, S. B.; Xuan, X. P. *J. Phys. Chem. B.* **2008**, *112*, 16682–16689.
(18) Wasserscheid, P.; Hal, R. V.; Andreas, B. *Green Chem.* **2002**, *4*, 400–404.
(19) Wilkes, J. S.; Zaworotko, M. J. *J. Chem. Soc., Chem. Commun* **1992**, 965–967.
(20) Waffenschmidt, H. Ph.D. Thesis, RWTH Aachen, 2000.
(21) Karodia, N.; Guise, S.; Newlands, C.; Andersen, J. A. *Chem Commun.* **1998**, 2341–2342.
(22) Alberto, A.; Héctor, R.; Ana, S. *Green Chem.* **2007**, *9*, 247–253.
(23) Harjani, J. R.; Farrell, J.; Garcia, M. T.; Singer, R. D.; Scammells, P. J. *Green Chem.* **2009**, *11*, 821–829.
(24) Miskolczy, Z.; Krisztina, S.-N.; László, B.; Sinem, G. *Chem. Phys. Lett.* **2004**, *400*, 296–300.
(25) Singh, T.; Drechsler, M.; Müeller, A. H. E.; Mukhopadhyay, I.; Kumar, A. *Phys. Chem. Chem. Phys.* **2010**, *12*, 11728–11735.
(26) Itoh, T.; Matsushita, Y.; Abe, Y.; Han, S. H.; Wada, S.; Hayase, S.; Kawatsura, M.; Takai, S.; Morimoto, M.; Hirose, Y. *Chem.—Eur. J.* **2006**, *12*, 9228–9237.
(27) Hang, X.; Peng, Y.; Zhao, K. S.; Xiao, J. X. *J. Chem. Eng. Data* **2011**, *56*, 865–873.
(28) Mukai, T.; Yoshio, M.; Kato, T.; Yoshizawaa, M.; Ohno, H. *Chem. Commun.* **2005**, 1333–1335.
(29) Hines, J. D.; Fragneto, G.; Thomas, R. K.; Garrett, P. R.; Rennie, G. K.; Rennie, A. R. *J. Colloid Interface Sci.* **1997**, *189*, 259–267.
(30) Lisi, R. D.; Inglese, S.; Milioto, P. *J. Colloid Interface Sci.* **1996**, *180*, 174–187.
(31) Zhao, G. X.; Zhu, B. Y. *Principles of Surfactant Action [M]*; China Light Industry Press: Beijing, China, 2003; p 115.
(32) Zhao, M. W.; Zheng, L. Q. *Phys. Chem. Chem. Phys.* **2011**, *13*, 1332–1337.
(33) Dong, B.; Zhao, X. Y.; Zheng, L. Q.; Zhang, J.; Li, N.; Inoue, T. *Colloids Surf., A* **2008**, *317*, 666–672.
(34) Muller, N. *Langmuir* **1993**, *9*, 96–100.
(35) Zana, R. *Langmuir* **1996**, *12*, 1208–1211.
(36) Zhang, H. C.; Li, K.; Liang, H. J.; Wang, J. J. *Colloids Surf., A* **2008**, *329*, 75–81.
(37) Behera, K.; Siddharth, P. *J. Colloid Interface Sci.* **2007**, *316*, 803–814.
(38) Freire, M. G.; Neves, C. M. S. S.; Carvalho, P. J.; Gardas, R. L.; Fernandes, A. M.; Marrucho, I. M.; Santos, L. M.; F., N. B.; Coutinho, J. A. P. *J. Phys. Chem. B* **2007**, *111*, 13082–13089.
(39) Anouti, M.; Jones, J.; Boisset, A.; Jacquemin, J.; Magaly, C.-C.; Lemordant, D. *J. Colloid Interface Sci.* **2009**, *340*, 104–111.
(40) Jaycock, M. J.; Parfitt, G. D. *Chemistry of Interfaces*; John Wiley and Sons: New York, 1981.
(41) Miki, K.; Westh, P.; Nishikawa, K.; Koga, Y. *J. Phys. Chem. B.* **2005**, *109*, 9014–9019.
(42) Anouti, M.; Jones, J.; Boisset, A.; Jacquemin, J.; Magaly, C.-C.; Lemordant, D. *J. Colloid Interface Sci.* **2009**, *340*, 104–111.
(43) Shi, L. J.; Li, N.; Yan, H.; Gao, Y. A.; Zheng, L. Q. *Langmuir* **2011**, *27* (5), 1618–1625.
(44) Shanks, P. C.; Franses, E. *J. Phys. Chem.* **1992**, *96*, 1794–1805.
(45) Rosen, M. J. *Surfactants and Interfacial Phenomena*, 2nd ed.; Wiley: New York, 1989.
(46) Hunter, R. J. *Foundations of Colloid Science*; Oxford University Press: New York, 1989; p 1.
(47) Inoue, T.; Ebina, H.; Dong, B.; Zheng, L. Q. *J. Colloid Interface Sci.* **2007**, *314*, 236–241.
(48) Shah, S. S.; Jamroz, N. U.; Sharif, Q. M. *Colloids Surf., A* **2001**, *178*, 199–206.
(49) Geng, F.; Liu, J.; Zheng, L. Q.; Yu, L.; Li, Z.; Li, G. Z.; Tung, C. H. *J. Chem. Eng. Data* **2010**, *55*, 147–151.
(50) Ao, M. Q.; Xu, G. Y.; Zhu, Y. Y.; Bai, Y. *J. Colloid Interface Sci.* **2008**, *326*, 495–495.
(51) Zana, R.; In, M.; Hélène, L. *Langmuir* **1997**, *13* (21), 5552–5557.
(52) Asakawa, T.; Kubode, H.; Ozawa, T.; Ohta, A.; Miyagishi, S. *J. Oleo Sci.* **2005**, *54*, 545–552.
(53) Lindman, B.; Söderman, O.; Wennerström, H. In *Surfactant Solutions: New Methods of Investigation*; Zana, R., Ed.; Marcel Dekker: New York, 1987; Chapter 6.
(54) Dieter, L.; Roberts, J. D. *J. Am. Chem. Soc.* **1973**, *95*, 4996–5003.
(55) Dávila, M. J.; Aparicio, S.; Alcalde, R.; García, B.; Leal, J. M. *Green Chem.* **2007**, *9*, 221–232.
(56) Chang, N. J.; Eric, W. K. *J. Phys. Chem.* **1985**, *89*, 2996–3000.